Thermal averaging of the indirect nuclear spin-spin coupling constants of ammonia: The importance of the large amplitude inversion mode

Andrey Yachmenev, Sergei N. Yurchenko, Ivana Paidarová, Per Jensen, Walter Thiel, and Stephan P. A. Sauer

Citation: J. Chem. Phys. **132**, 114305 (2010); doi: 10.1063/1.3359850
View online: https://doi.org/10.1063/1.3359850
View Table of Contents: http://aip.scitation.org/toc/jcp/132/11
Published by the American Institute of Physics

Thermal averaging of the indirect nuclear spin-spin coupling constants of ammonia: The importance of the large amplitude inversion mode

Andrey Yachmenev,[1] Sergei N. Yurchenko,[2] Ivana Paidarová,[3] Per Jensen,[4] Walter Thiel,[1] and Stephan P. A. Sauer[5,a)]

[1]*Max-Planck-Institut für Kohlenforschung, Kaiser-Wilhelm-Platz 1, D-45470 Mülheim an der Ruhr, Germany*
[2]*Physikalische Chemie, Technische Universität Dresden, Mommsenstr. 13, D-01062 Dresden, Germany*
[3]*J. Heyrovský Institute of Physical Chemistry, Academy of Sciences of the Czech Republic, Dolejškova 3, CZ 182 23 Praha 8, Czech Republic*
[4]*Fachbereich C-Theoretische Chemie, Bergische Universität, D-42097 Wuppertal, Germany*
[5]*Department of Chemistry, University of Copenhagen, Universitetsparken 5, DK-2100 Copenhagen Ø, Denmark*

(Received 25 January 2010; accepted 22 February 2010; published online 18 March 2010)

Analytic internal-coordinate representations are reported for two accurate *ab initio* spin-spin coupling surfaces of the ammonia molecule, ^1J (^{15}N,H) and ^2J(H,H). Calculations were carried out at the level of the second-order polarization propagator approximation involving coupled-cluster singles and doubles amplitudes (CCSD) and using a large specialized basis set, for a total of 841 different geometries corresponding to 2523 distinct points on the ^1J (^{15}N,H) and ^2J(H,H) surfaces. The results were fitted to power series expansions truncated after the fourth-order terms. While the one-bond nitrogen-hydrogen coupling depends more on the internuclear distance, the geminal hydrogen-hydrogen coupling exhibits a pronounced dependence on the bond angle. The spin-spin parameters are first vibrationally averaged, using vibrational wave functions obtained variationally from the TROVE computer program with a CCSD(T) based potential energy surface, for ammonia and its various deuterated isotopologues. The vibrationally averaged quantities are then thermally averaged to give values of the couplings at absolute temperatures of 300 and 600 K. We find that the nuclear-motion corrections are rather small. The computed one-bond couplings and their minute isotope effects are in excellent agreement with the experimental values. © *2010 American Institute of Physics*. [doi:10.1063/1.3359850]

I. INTRODUCTION

Accurate calculations of nuclear magnetic resonance indirect nuclear spin-spin coupling constants J have long been a challenge for theoretical chemistry.[1–3] The form of the one-electron operators for the interaction between the nuclear spin and the electrons—in particular the Fermi contact (FC) operator, which measures the spin density at the position of the nucleus, and the paramagnetic nuclear spin–electronic orbit (PSO) operator, which includes the electronic angular momentum operator—makes it necessary to use specially optimized basis sets.[4–14] Furthermore the FC and spin-dipolar (SD) contributions are obtained, in principle, as sums over excited triplet states for a closed shell molecule, and this requires a considerable amount of electron correlation to be included in the calculation. Self-consistent-field (SCF) linear response calculations often suffer from triplet instabilities or quasi-instabilities,[6,8,15–22] which renders SCF results for J unreliable. This happens in particular for systems with many lone-pairs or π-electrons, but can be overcome in sufficiently correlated wave function methods. Also density functional theory (DFT) with standard functionals has problems with reproducing spin-spin coupling constants for atoms with several lone-pairs such as fluorine.[23–26]

Nevertheless, with appropriate basis sets and correlated methods such as the second order polarization propagator approximation with coupled cluster singles and doubles amplitudes [SOPPA(CCSD)] method,[6,27] multiconfigurational self-consistent field linear response theory (MCSCF-LR)[28,29] using wave functions with sufficiently large active spaces or coupled cluster methods,[30–35] the calculations become sufficiently accurate that minor effects such as relativistic corrections and the influence of nuclear motion determine the remaining errors. The influence of molecular vibrations on the spin-spin coupling constants has therefore been the topic of several studies using SOPPA(CCSD),[36–49] MCSCF-LR,[29,44,50–52] or even DFT.[53–55] Zero-point vibrational corrections to one-bond X–H (X=C, O, F, Si) coupling constants amount typically to 5% whereas the corrections to geminal H–H coupling constants can be even larger. Small changes in the coupling constants of CH_4,[42,56,57] H_2O,[43,52,57] HF,[51] C_2H_2,[45,47] and SiH_4 (Refs. 49 and 57) such as isotope effects or temperature dependence can be reproduced in this way.

These calculations require the value of the spin-spin coupling constants not only for a single nuclear conformation, but for a particular vibrational state, and this implies that the

a)Author to whom correspondence should be addressed. Electronic mail: sauer@kiku.dk.

spin-spin coupling constant as a function of the internal nuclear coordinates has to be averaged over the corresponding vibrational wave function. This can be done either directly by numerically averaging the coupling constant surface over numerical vibrational wave functions[36,44] or by first performing a Taylor expansion of the coupling constant surface around the equilibrium geometry to a given order in internal[37,42,43,45,47,49] or normal coordinates[29,50–54] to facilitate the averaging over the vibrational wave functions. The Taylor expansion is typically truncated after the quadratic terms such that only first and second derivatives of the coupling constants at the equilibrium geometry are needed. The vibrational wave functions are normally obtained by first order perturbation theory with the exception of one recent study[55] which employed several variational methods.

NH_3 is obviously missing in the list of recent vibrational-averaging calculations employing high level wave function methods. It differs from most of the other molecules studied so far in having a large amplitude inversion mode that cannot be treated appropriately by perturbation theory. The two symmetric isotopologues NH_3 and ND_3 can be handled by the nonrigid invertor method of Špirko and co-workers.[58,59] Using this approach, vibrationally averaged values of several other molecular properties of ammonia have been obtained,[60–65] but the spin-spin coupling constants have not been calculated. However, the nonrigid invertor method was employed in the calculation of vibrationally averaged spin-spin coupling constants of the oxonium ion.[44]

On the other hand, the perturbation-theory approach was applied to the spin-spin coupling constants of ammonia in a recent DFT study[53] and in two older studies.[66,67] Kowalewski and Roos[66] employed a configuration interaction singles and doubles wave function with a basis set of double zeta plus polarization quality and studied only corrections to the geminal H–H coupling constant from the two totally symmetric vibrational modes. As vibrational wave functions for the two symmetric modes, they used linear combinations of products of Hermite functions. They observed that the geminal hydrogen coupling constant becomes increasingly negative upon inclusion of vibrational corrections. Solomon and Schulman[67] studied the N–H as well as the H–H coupling but only at the semi-empirical intermediate neglect of differential overlap (INDO) level. In the vibrational averaging, they considered all normal modes and expressed the vibrational wave functions as products of harmonic oscillator wave functions apart from the inversion mode, which they treated numerically. This implies that they neither included the couplings between the modes nor the contributions from the anharmonic force constants. They found that the calculated zero-point vibrational corrections depend strongly on the kind of wave function used for the inversion mode. Employing harmonic oscillator wave functions they obtained a zero-point vibrational correction for the geminal hydrogen coupling similar to that of Kowalewski and Roos,[66] whereas treating the inversion mode numerically reduces the zero-point vibrational correction by more than 50%. For the nitrogen-hydrogen one-bond coupling, they observed a similar strong dependence on the chosen treatment of the inversion mode, but here the zero-point vibrational correction more than doubles when the inversion mode is treated numerically. In any case, they find that the one-bond nitrogen-hydrogen coupling constant also becomes increasingly negative upon inclusion of vibrational corrections. Finally, Ruden *et al.*[53] employed not only zeroth order vibrational wave functions expressed as products of harmonic oscillator wave functions, but also the first order wave functions which account for couplings between vibrational modes and contributions from the anharmonic force constants. The inversion mode, however, was treated like the other vibrational modes. The necessary spin-spin coupling constant geometrical derivatives as well as the force constants were calculated at the DFT level employing the B3LYP functional and a basis set optimized for the calculation of coupling constants. Contrary to the previous studies Ruden *et al.*[53] found that the zero-point vibrational corrections to both couplings are positive and that in the case of the one-bond nitrogen-hydrogen coupling, the zero-point vibrational correction is an order of magnitude smaller than the value of Solomon and Schulman.[67]

In view of the above, we have reinvestigated the vibrational corrections to the coupling constants in ammonia using state-of-the-art correlated wave function methods. Contrary to earlier studies, we have not employed perturbation theory in the calculation of the vibrational corrections, but have for the first time directly averaged the multidimensional coupling constant surfaces obtained at the SOPPA(CCSD) level using accurate rovibrational wave functions. The latter were determined by means of the variational approach TROVE[68] in conjunction with a highly accurate potential energy surface of ammonia by Yurchenko *et al.*[69] For the averaging, the matrix exponential technique[70] was implemented in TROVE and utilized. In the following, the averaging over rovibrational states will be referred to as "thermal averaging," indicating that we use all rovibrational states populated according to the Boltzmann distribution at $T=300$ and 600 K. In the present work we have only considered the spin-spin coupling constant, i.e., the trace of the spin-spin coupling tensor. However, the same approach could be applied to all tensor elements in order to obtain the thermally averaged anisotropy of the coupling constants.

Finally, we note that the vapor-to-liquid shift of the coupling constants in NH_3 has been studied very recently by Gester *et al.*[71] employing a sequential QM/MM approach at the DFT(B3LYP) level of theory. For the experimentally inaccessible $^2J(\mathrm{H},\mathrm{H})$ parameter in NH_3, a shift of -2.5 Hz was predicted, whereas the shift for ^1J $(^{15}\mathrm{N},\mathrm{H})$ was computed to be 0.5 Hz, i.e., very small when compared to the results of a similar recent study on water.[72]

The paper is structured as follows. In Sec. II we discuss first the values of the spin-spin coupling constants at the equilibrium geometry before we consider the effects of averaging in Sec. III.

II. ELECTRONIC STRUCTURE CALCULATIONS

A. Computational details

It has been described many times (see, for example, Refs. 1 and 73) how to calculate the four Ramsey[74] contributions (FC, SD, paramagnetic, and diamagnetic spin-orbit) to the indirect nuclear spin-spin coupling constants using response theory methods.[73,75] The linear response functions employed in the present work were either based on MCSCF wave functions,[28,29] or they were obtained from Møller–Plesset perturbation theory as implemented in the SOPPA(CCSD) method[6,27] and in its parent method, the SOPPA.[6,76–79] The MCSCF wave functions were either of the complete active space (CAS) type[80] or of the restricted active space (RAS) type.[81] The choice of active orbitals (2–6 a_1 and 1–4 e) in the CAS calculation and (2–10 a_1 and 1–4 e in RAS 2, 11–13 a_1, and 5–7 e in RAS 3 with singles and doubles excitations from RAS 2 to RAS 3) in the RAS calculation was based on the natural orbital occupation numbers of a second order Møller–Plesset (MP2) calculation.[82,83] Both MCSCF calculations were started from the MP2 natural orbitals calculated with the inactive orbitals of the MCSCF calculation kept frozen. In all calculations, the diamagnetic spin-orbit (DSO) contribution was obtained not as a linear response function[84] but as a ground state average value. At the SOPPA and SOPPA(CCSD) level of theory, this involves the same unrelaxed one-density matrix as used elsewhere in the SOPPA and SOPPA(CCSD) approaches.[27,85] All electronic structure calculations were carried out with the 2.0 version of the DALTON program package.[6,27,29,78,86–88]

Accurate calculations of spin-spin coupling constants require either very large standard basis sets or smaller, specially optimized basis sets. We have used the second option in this work, as we need to calculate a whole coupling constant surface. The coupling constants in ammonia are similar to those of water and methane in that they are dominated by the Fermi-contact contribution, which can only be calculated accurately with extra tight s-type functions in the basis set. The basis set for hydrogen was taken from the previous study of the spin-spin coupling constants of H_2O,[43] whereas a new nitrogen basis set was devised, corresponding to the oxygen basis set used in Ref. 43. The chosen basis set consists of 17s-, 7p-, 5d-, and 2f-type primitive spherical Gaussian functions for nitrogen and of 11s-, 2p-, and 2d-type primitive spherical Gaussian functions for hydrogen. The s-type functions for nitrogen were taken from van Duijneveldt's[89] 13s8p basis set and were augmented by one diffuse (with exponent $\zeta_s=0.055\,555$) and three tight functions (with exponents $\zeta_s=502\,471.053\,087$, 3 377 091.588 02, and 22 697 322.6095), whereas the p-type functions are from van Duijneveldt's[89] 13s7p basis set. The polarization functions for nitrogen are from Dunning's[90] 3d2f basis set augmented by two tight d-type functions with exponents $\zeta_d=2.837$ and 8.315. The s-type functions for hydrogen are van Duijneveldt's[89] 7s basis set augmented by four tight s-type functions with exponents $\zeta_s=1258.122\,088$, 8392.099 358, 55 978.137 820, and 373 393.090 348. The polarization functions for hydrogen are Dunning's[90] 2p and 2d basis sets.

B. Calculations at equilibrium geometry

Tables I and II give values for ^1J (^{15}N,H) and ^2J(H,H), and for the various terms contributing to them, for the ammonia molecule at equilibrium geometry. Our MCSCF, SOPPA, and SOPPA(CCSD) values are compared with results from a selection of earlier papers.[1,9,30,34,53,57,66,67,71,91–97] We note that there is perfect agreement between the results of our SOPPA(CCSD) and the computationally much more demanding $^{10}RAS^{94}_{33SD}$ calculations for both coupling constants. This is in line with earlier findings[43–45] and supports our choice of SOPPA(CCSD) for calculating the coupling constant surfaces. Furthermore, the SOPPA results are in closer agreement with the SOPPA(CCSD) and $^{10}RAS^{94}_{33SD}$ results than the $^{10}CAS^{54}$ results. This underlines the importance of dynamical correlation effects involving many more orbitals than the ones normally included in the CAS approach for the calculation of spin-spin coupling constants.

Finally, we find that in general, our results compare well with the results of earlier correlated calculations. Some of the differences can be attributed to differences in the chosen geometry. This is, for example, the case when we compare the present results with those from earlier SOPPA calculations.[34] Many calculations, including the present ones, were done at the experimental equilibrium geometry [$r_{NH}=1.0124$ Å, $\angle$(HNH)$=106.67°$][98] while some of the earlier studies employed a slightly shorter bond length (1.0116–1.012 Å)[34,66,71] and a wider bond angle [$\angle$(HNH)$=107.10°$ or $\angle$(HNH)$=108.067°$].[34,71] Other calculations were done at optimized geometries.[53,94,96,97] Another more important reason for the deviations is the difference in basis sets. Specialized basis sets were only employed in some of the more recent studies.[9,53,57,71,94–96] Generally speaking, however, there is very good agreement between the best previous and present results (keeping in mind the subtle differences in geometry).

Tables I and II show that both couplings are dominated by the FC contribution. However, in order to calculate the one-bond ^1J (^{15}N,H) coupling constant accurately, it is necessary to include also the PSO contribution, which amounts to about 5% of the total coupling constant. Similarly, the sum of the PSO and DSO terms contributes about 10% of the geminal ^2J(H,H) coupling constant. In this respect, ammonia behaves like the other second row hydrides.[42,43] Electron correlation reduces the FC contribution to ^1J (^{15}N,H) and ^2J(H,H) by ~21% and ~54%, respectively, while the changes in the other contributions are negligible.

To generate the vibrational wave functions used in the vibrational averaging (see below) we employ the CCSD(T)-based spectroscopic potential energy surface of $^{14}NH_3$ from Ref. 69, with the equilibrium geometry at $r_{NH}=1.0103$ Å and $\angle$(HNH)$=106.72°$. The nuclear eigenfunctions are obtained as the variational solution of the rovibrational Schödinger equation on this potential energy surface. The corresponding equilibrium values of ^1J (^{15}N,H) and ^2J(H,H), also given in Tables I and II, serve as reference points for calculating the vibrational and thermal effects on these properties. It should be noted that the choice of the equilibrium geometry does affect the one-bond ^1J (^{15}N,H) coupling constant: the change from the experimental to the

TABLE I. Calculated nitrogen-proton coupling constants, ^1J (^{15}N,H), of ammonia at equilibrium geometry. All values are in Hz and are presented in order of the date of publication.

Method	Basis set	Ref.	r_{NH} (Å)	∠(HNH)	$^1J_{eq}^{FC}$	$^1J_{eq}^{SD}$	$^1J_{eq}^{DSO}$	$^1J_{eq}^{PSO}$	$^1J_{eq}$
INDO	n/a	67	1.0136	106.67°	⋯	⋯	⋯	⋯	−35.01
SOS-CI	6–31G	91	Not specified		−72.28	0.08	−0.19	−2.51	−74.91
SCF	6–311G**	92	1.0124	106.67°	−63.60	0.03	−0.10	−2.86	−66.54
EOM	6–311G**	92	1.0124	106.67°	−54.10	−0.02	−0.10	−2.47	−56.68
SCF	Varying[a]	93	1.012 395	106.67°	−63.29	0.07	−0.10	−2.57	−65.89
FF-MBPT[2]	Varying[a]	93	1.012 395	106.67°	−57.54	0.04	−0.11	−2.44	−60.07
SCF	Nonstandard[b]	30	1.012 395	106.67°	−71.53	0.04	−0.10	−2.45	−74.04
EOM-CCSD	Nonstandard[b]	30	1.012 395	106.67°	−56.38	−0.10	−0.11	−2.06	−58.65
^{10}CAS^{94} SCF	HuzIV	1	Experimental		−56.25	⋯	⋯	⋯	−59.27
DFT/B3LYP	HuzII-su3	94	Optimized		⋯	⋯	⋯	⋯	−63.70
^{10}RAS$^{52}_{14,8SD}$ SCF	HuzIII-su4	95	1.0124	106.67°	−58.05	−0.13	−0.08	−2.86	−61.15
^{10}CAS^{94} SCF	aug-cc-pVQZ-su1	96	Optimized		⋯	⋯	⋯	⋯	−61.70
^{10}CAS^{52} SCF	aug-cc-pVTZ	97	Optimized		⋯	⋯	⋯	⋯	−61.84
DFT/B3LYP	HuzIII-su3	53	Optimized		⋯	⋯	⋯	⋯	−64.10
DFT/B3LYP	cc-pCV5Z-sd+t	9	1.0124	106.67°	−60.7	−0.3	0.0	−3.2	−64.4
SOPPA	qzp/qz2p	34	1.0117	108.067°	⋯	⋯	⋯	⋯	−63.9
EOM-CCSD	qzp/qz2p	34	1.0117	108.067°	⋯	⋯	⋯	⋯	−61.5
SOPPA(CCSD)	aug-cc-pVTZ-Juc	57	1.0124	106.67°	⋯	⋯	⋯	⋯	−61.59
DFT/B3LYP	aug-cc-pVTZ-J	71	1.012	107.10°	−60.75	−0.24	−0.07	−3.10	−64.37
SCF	This work		1.0124	106.67°	−75.22	−0.02	−0.06	−3.07	−78.37
^{10}CAS^{54} SCF	This work		1.0124	106.67°	−60.8	−0.17	−0.07	−2.91	−63.95
^{10}RAS$^{94}_{33SD}$ SCF	This work		1.0124	106.67°	−58.98	−0.18	−0.07	−2.93	−62.17
SOPPA	This work		1.0124	106.67°	−59.28	−0.15	−0.07	−2.94	−62.43
SOPPA(CCSD)	This work		1.0124	106.67°	−58.87	−0.18	−0.07	−2.97	−62.09
SOPPA[c]	This work		1.0103	106.72°	⋯	⋯	⋯	⋯	−62.31

[a]Basis set: 6–311G** (FC), 6–31G (SD), 6–31G** (OP, OD).
[b]Basis set: N: (10s6p1d)→[6s3p1d], H: (6s1p)→[4s1p].
[c]SOPPA(CCSD) value at the reference equilibrium geometry (see text).

CCSD(T) equilibrium geometry results in a difference of 0.22 Hz which, as will be seen below, is almost as large as the vibrational correction.

C. Spin-spin coupling surfaces

Taking into account the symmetry of NH_3, it can be shown that the six spin-spin coupling constant surfaces ^1J (^{15}N,H$_i$), $i=1,2,3$ and ^2J(H$_i$,H$_j$), $i<j=1,2,3$ can be given in terms of two single functions $^1\bar{J}^{N1}(r_1,r_2,r_3,\alpha_{23},\alpha_{13},\alpha_{12})$ and $^2\bar{J}^{23}(r_1,r_2,r_3,\alpha_{23},\alpha_{13},\alpha_{12})$,

$$^1J(^{15}\mathrm{N},\mathrm{H}_1) = {}^1\bar{J}^{N1}(r_1,r_2,r_3,\alpha_{23},\alpha_{13},\alpha_{12}) = {}^1\bar{J}^{N1}(r_1,r_3,r_2,\alpha_{23},\alpha_{12},\alpha_{13}), \quad (1)$$

$$^1J(^{15}\mathrm{N},\mathrm{H}_2) = {}^1\bar{J}^{N1}(r_2,r_3,r_1,\alpha_{13},\alpha_{12},\alpha_{23}) = {}^1\bar{J}^{N1}(r_2,r_1,r_3,\alpha_{13},\alpha_{23},\alpha_{12}), \quad (2)$$

$$^1J(^{15}\mathrm{N},\mathrm{H}_3) = {}^1\bar{J}^{N1}(r_3,r_1,r_2,\alpha_{12},\alpha_{23},\alpha_{13}) = {}^1\bar{J}^{N1}(r_3,r_2,r_1,\alpha_{12},\alpha_{13},\alpha_{23}), \quad (3)$$

and

$$^2J(\mathrm{H}_2,\mathrm{H}_3) = {}^2\bar{J}^{23}(r_1,r_2,r_3,\alpha_{23},\alpha_{13},\alpha_{12}) = {}^2\bar{J}^{23}(r_1,r_3,r_2,\alpha_{23},\alpha_{12},\alpha_{13}), \quad (4)$$

$$^2J(\mathrm{H}_1,\mathrm{H}_3) = {}^2\bar{J}^{23}(r_2,r_3,r_1,\alpha_{13},\alpha_{12},\alpha_{23}) = {}^2\bar{J}^{23}(r_2,r_1,r_3,\alpha_{13},\alpha_{23},\alpha_{12}), \quad (5)$$

$$^2J(\mathrm{H}_1,\mathrm{H}_2) = {}^2\bar{J}^{23}(r_3,r_1,r_2,\alpha_{12},\alpha_{23},\alpha_{13}) = {}^2\bar{J}^{23}(r_3,r_2,r_1,\alpha_{12},\alpha_{13},\alpha_{23}). \quad (6)$$

These functions $^1\bar{J}^{N1}$ and $^2\bar{J}^{23}$ are expressed as expansions

$$^{1/2}\bar{J}^{N1/23} = {}^{1/2}\bar{J}_0^{N1/23} + \sum_k^6 F_k\xi_k + \sum_{k\le l}^6 F_{k,l}\xi_k\xi_l + \sum_{k\le l\le m}^6 F_{k,l,m}\xi_k\xi_l\xi_m + \sum_{k\le l\le m\le n}^6 F_{k,l,m,n}\xi_k\xi_l\xi_m\xi_n \quad (7)$$

in the variables

$$\xi_k = \Delta r_k = r_k - r_e, \quad k=1,2,3, \quad (8)$$

$$\xi_4 = \Delta\alpha_{23} = \alpha_{23} - \alpha_e, \quad (9)$$

TABLE II. Calculated proton-proton coupling constants, $^2J(\mathrm{H,H})$, of ammonia at equilibrium geometry. All values are in Hz and are presented in order of the date of publication.

Method	Basis set	Ref.	r_{NH} (Å)	∠(HNH)	$^2J_{eq}^{FC}$	$^2J_{eq}^{SD}$	$^2J_{eq}^{DSO}$	$^2J_{eq}^{PSO}$	$^2J_{eq}$
CISD	Nonstandard[a]	66	1.0116	106.7°	⋯	⋯	⋯	⋯	−6.83
INDO	n/a	67	1.0136	106.67°	⋯	⋯	⋯	⋯	−7.88
SOS-CI	6–31G	91	Not specified		−28.92	1.39	−5.12	1.98	−30.33
SCF	6–311G**	92	1.0124	106.67°	−23.91	0.69	−5.2	5.06	−23.37
EOM	6–311G**	92	1.0124	106.67°	−14.78	0.49	−5.2	4.71	−14.78
SCF	Varying[b]	93	1.012 395	106.67°	−23.93	1.05	−5.25	4.46	−23.67
FF-MBPT[2]	Varying[b]	93	1.012 395	106.67°	−20.05	0.95	−5.2	4.39	−19.9
SCF	Nonstandard[c]	30	1.012 395	106.67°	−23.6	0.78	−5.22	4.49	−23.55
EOM-CCSD	Nonstandard[c]	30	1.012 395	106.67°	−11.72	0.55	−5.13	4.21	−12.09
^{10}CAS^{94} SCF	HuzIV	1	Experimental		−11.21	⋯	⋯	⋯	−9.77
DFT/B3LYP	HuzII-su3	94	Optimized		⋯	⋯	⋯	⋯	−9.8
^{10}RAS$^{52}_{14,8SD}$ SCF	HuzIII-su4	95	1.0124	106.67°	−12.51	0.62	−5.19	5.74	−11.33
^{10}CAS^{94} SCF	aug-cc-pVQZ-su1	96	Optimized		⋯	⋯	⋯	⋯	−11.4
^{10}CAS^{52} SCF	aug-cc-pVTZ	97	Optimized		⋯	⋯	⋯	⋯	−15.45
DFT/B3LYP	HuzIII-su3	53	Optimized		⋯	⋯	⋯	⋯	−10.1
DFT/B3LYP	cc-pCV5Z-sd+t	9	1.0124	106.67°	−11.8	0.7	−5.3	6.4	−10.0
DFT/B3LYP	aug-cc-pVTZ-J	71	1.012	107.10°	−11.82	0.6	−5.25	6.15	−10.32
SCF	This work		1.0124	106.67°	−26.3	0.91	−5.29	6.24	−24.44
^{10}CAS^{54} SCF	This work		1.0124	106.67°	−13.76	0.7	−5.23	6.17	−12.11
^{10}RAS$^{94}_{33SD}$ SCF	This work		1.0124	106.67°	−12.82	0.68	−5.23	6.19	−11.18
SOPPA	This work		1.0124	106.67°	−13.54	0.68	−5.25	6.26	−11.86
SOPPA(CCSD)	This work		1.0124	106.67°	−12.94	0.67	−5.24	6.24	−11.27
SOPPA[d]	This work		1.0103	106.72°	⋯	⋯	⋯	⋯	−11.24

[a]Basis set: N: (9s5p1d)→[4s2p1d], H: (5s1p)→[3s1p].
[b]Basis set: 6–311G** (FC), 6–31G (SD), 6–31G** (OP, OD).
[c]Basis set: N: (10s6p1d)→[6s3p1d], H: (6s1p)→[4s1p].
[d]SOPPA(CCSD) value at the reference equilibrium geometry (see text).

$$\xi_5 = \Delta\alpha_{13} = \alpha_{13} - \alpha_e, \tag{10}$$

$$\xi_6 = \Delta\alpha_{12} = \alpha_{12} - \alpha_e. \tag{11}$$

Here, r_i is the instantaneous value of the distance between the central N nucleus and H_i, where H_i is the proton labeled i (=1, 2, or 3); α_{ij} denotes the bond angle $\angle(H_iNH_j)$. The quantities r_e=1.0103 Å and α_e=106.72° (Ref. 69) are the equilibrium values of the r_i and α_{ij}, respectively, chosen as expansion centers for the series expansions representing ^1J (^{15}N,H) and ^2J(H,H).

The expansion coefficients $F_{k,l,m,\ldots}$ in Eq. (7) obey the following permutation rules:

$$F_{k',l',m',\ldots} = F_{k,l,m,\ldots}, \tag{12}$$

when the indices $k',l',m',\ldots$ are obtained from $k,l,m,\ldots$ by replacing all indices 2 by 3, all indices 3 by 2, all indices 5 by 6, and all indices 6 by 5. All six coupling constants were calculated at the SOPPA(CCSD) level of theory for 841 different nuclear arrangements of $^{15}NH_3$, which gave 2523 points on the $^1\bar{J}^{N1}$ and $^2\bar{J}^{23}$ surfaces. The values of the expansion parameters in Eq. (7) were obtained in a least-squares fitting to the points on the two coupling surfaces. For the $^1\bar{J}^{N1}$ and $^2\bar{J}^{23}$ functions we could usefully vary 75 and 79 parameters, respectively, which had root-mean-square (rms) deviations of 0.08 and 0.06 Hz. Tables III and IV list the optimized parameter values. Parameters, whose absolute values were determined to be less than their standard errors in initial fittings, were constrained to zero in the final fitting and omitted from the table. Furthermore, we give in the tables only one member of each parameter pair related by Eq. (12). The optimized parameters are given as supplementary material together with a FORTRAN routine for evaluating the $^1\bar{J}^{N1}$ and $^2\bar{J}^{23}$ values at arbitrary geometries.[99]

Analyzing the linear and quadratic coefficients, we find that the one-bond nitrogen-hydrogen couplings $^1\bar{J}^{N1}$ depend more strongly on the length of the bond between the two coupled atoms ($^1J_r^{NH}$=81.2396 Hz Å^{-1}) than on any of the other bond lengths ($^1J_s^{NH}$=−9.6375 Hz Å^{-1}). This confirms that unlike methane and silane,[42,46,48,49,56,57] ammonia does not exhibit an unusual differential sensitivity.[38] Furthermore, the expansion coefficients for the one-bond nitrogen-hydrogen couplings, $^1\bar{J}^{N1}$, are quite large for the "associated" bond lengths ($^1J_r^{NH}$=81.2396 Hz Å^{-1} and $^1J_{rr}^{NH}$=81.22 Hz Å^{-2}) but somewhat smaller for the angle to the neighboring H atom ($^1J_\alpha^{NH}$=−45.4271 Hz rad^{-1} and $^1J_{\alpha\alpha}^{NH}$=−61.878 Hz rad^{-2}). The opposite is true for the geminal hydrogen-hydrogen couplings, $^2\bar{J}^{23}$, where geometry dependence is dominated by the bond angle terms involving the parameters $^2J_\alpha^{HH}$ and $^2J_{\alpha\alpha}^{HH}$. A similar behavior was previously observed for other magnetic properties of ammonia[62,64] and of the isoelectronic H_3O^+ ion.[44,100]

TABLE III. Expansion coefficients of the calculated nitrogen-proton coupling constant surface, ^1J (^{15}N,H), of the ammonia molecule defined in Eq. (7). Derivatives involving the bond length changes Δr_i have been obtained with these coordinates in Å. Derivatives involving the angular variations $\Delta\alpha_{ij}$ have been obtained with these coordinates in radians. Coupling constants are in Hz.

Parameter	Value	Parameter	Value	Parameter	Value
$^1\bar{J}_0^{N1}$	−62.308 62	F_{135}	86.0	F_{1146}	−396.
$F_1=^1J_r^{NH}$	81.2396	F_{144}	−18.5	F_{1155}	88.
$F_3=^1J_s^{NH}$	−9.6375	F_{146}	9.7	F_{1156}	−48.0
$F_4=^1J_\gamma^{NH}$	−9.5986	F_{155}	−83.7	F_{1222}	−64.0
$F_5=^1J_\alpha^{NH}$	−45.4271	F_{156}	−248.8	F_{1225}	52.
$F_{11}=\frac{1}{2}{}^1J_{rr}^{NH}$	40.61	F_{223}	26.03	F_{1233}	−19.
$F_{13}=^1J_{rs}^{NH}$	44.05	F_{226}	49.11	F_{1234}	114.
$F_{14}=^1J_{r\gamma}^{NH}$	−46.57	F_{234}	68.7	F_{1244}	−178.3
$F_{16}=^1J_{r\alpha}^{NH}$	−61.51	F_{245}	−148.40	F_{1445}	−590.
$F_{23}=^1J_{st}^{NH}$	10.82	F_{255}	−9.78	F_{1456}	170.
$F_{33}=\frac{1}{2}{}^1J_{ss}^{NH}$	31.854	F_{333}	12.76	F_{1466}	122.
$F_{34}=^1J_{s\gamma}^{NH}$	−22.02	F_{444}	2.64	F_{2222}	−13.8
$F_{35}=^1J_{s\alpha}^{NH}$	25.71	F_{445}	−12.85	F_{2224}	12.
$F_{36}=^1J_{s\beta}^{NH}$	−12.28	F_{456}	−59.98	F_{2225}	17.2
$F_{44}=\frac{1}{2}{}^1J_{\gamma\gamma}^{NH}$	−6.879	F_{466}	−20.10	F_{2244}	14.0
$F_{46}=^1J_{\alpha\gamma}^{NH}$	−24.624	F_{555}	−18.89	F_{2334}	76.
$F_{55}=\frac{1}{2}{}^1J_{\alpha\alpha}^{NH}$	−30.939	F_{556}	−33.39	F_{2444}	−353.7
$F_{56}=^1J_{\alpha\beta}^{NH}$	−33.154			F_{3666}	−13.4
		F_{1111}	604.5	F_{4445}	−1.45
F_{111}	−272.61	F_{1112}	−21.4	F_{4456}	−24.3
F_{112}	40.60	F_{1114}	−58.	F_{4466}	−21.8
F_{114}	−68.6	F_{1115}	39.8	F_{4555}	−13.1
F_{115}	−11.89	F_{1122}	11.5	F_{4556}	−43.2
F_{123}	60.9	F_{1123}	53.	F_{5566}	−39.6
F_{124}	−55.2	F_{1126}	82.	F_{5666}	−11.5
F_{133}	10.78	F_{1144}	−30.1		

III. THERMAL AVERAGING

A. Theory

We have used the variational program TROVE[68] for vibrational and thermal averaging of the spin-spin constants of 15-ammonia and its isotopologues $^{15}ND_3$, $^{15}NH_2D$, and $^{15}NH_2D$. The TROVE Hamiltonian is defined by the expansions of its kinetic-energy and potential-energy parts in terms of the internal coordinates. The coordinates and the expansion orders used presently are the same as in Ref. 101. The expansions of $G_{\lambda\mu}$ and U (see Ref. 68) around the nonrigid reference configuration are truncated after the sixth-order terms while the expansion of V is truncated after the eighth-order terms. The size of the basis set is controlled by the polyad number

$$P = 2(n_1 + n_2 + n_3) + n_4 + n_5 + n_6/2, \tag{13}$$

where the quantum numbers n_i are defined in connection with the primitive basis functions ϕ_{n_i}.[68] They are essentially the principal quantum numbers associated with the local-mode vibrations of NH_3. The basis set contains only products of primitive functions ϕ_{n_i} for which $P \leq P_{max}$. We found that the thermal averages were converged to better than 0.002% when using $P_{max}=10$. In the TROVE calculations, we used the spectroscopic potential energy surface of $^{14}NH_3$ from Ref. 69, which was generated by refining a CCSD(T) surface by fitting to available experimental vibrational energies.

For an ensemble of molecules in thermal equilibrium at absolute temperature T, the thermal average of an operator P is given by

$$\langle P\rangle_T = \frac{1}{Q}\sum_i g_i \exp\left(-\frac{E_{rv}^{(i)}}{kT}\right)\langle P\rangle_i, \tag{14}$$

where g_i is the degeneracy of the ith state with the energy $E_{rv}^{(i)}$ relative to the ground state energy, k is the Boltzmann constant, Q is the internal partition function defined as

$$Q = \sum_i g_i \exp\left(-\frac{E_{rv}^{(i)}}{kT}\right), \tag{15}$$

and $\langle P\rangle_i$ is an expectation value of the operator P in a rovibrational state i

$$\langle P\rangle_i = \langle \Phi_{rv}^{(i)}|P|\Phi_{rv}^{(i)}\rangle. \tag{16}$$

The calculation of the quantities in Eqs. (14)–(16) requires the eigenvalues $E_{rv}^{(i)}$ and eigenvectors $\Phi_{rv}^{(i)}$ which are usually obtained variationally, that is, by matrix diagonalization. Here we explore an alternative approach based on the matrix exponent technique,[70] in which we avoid a time-consuming diagonalization procedure. This approach is based on the realization that Eq. (14) represents the trace of a matrix product,

TABLE IV. Expansion coefficients of the calculated proton-proton coupling constant surface, $^2J(\mathrm{H,H})$, of the ammonia molecule defined in Eq. (7). Derivatives involving the bond length changes Δr_i have been obtained with these coordinates in Å. Derivatives involving the angular variations $\Delta\alpha_{ij}$ have been obtained with these coordinates in radians. Coupling constants are in Hz.

Parameter	Value	Parameter	Value	Parameter	Value
$^2\bar{J}_0^{23}$	−11.236 05	F_{144}	10.94	F_{1222}	−34.7
$F_1=^2J_t^{\mathrm{HH}}$	3.9149	F_{146}	43.7	F_{1233}	−14.8
$F_3=^2J_r^{\mathrm{HH}}$	0.8634	F_{155}	−11.75	F_{1234}	−103.
$F_4=^2J_\alpha^{\mathrm{HH}}$	48.3273	F_{156}	−2.8	F_{1244}	56.4
$F_5=^2J_\beta^{\mathrm{HH}}$	−0.4534	F_{223}	−24.67	F_{1444}	17.9
$F_{11}=\frac{1}{2}{}^2J_{tt}^{\mathrm{HH}}$	−0.080	F_{225}	19.86	F_{1445}	487.
$F_{13}=^2J_{rt}^{\mathrm{HH}}$	7.109	F_{226}	88.10	F_{1456}	−473.
$F_{14}=^2J_{t\alpha}^{\mathrm{HH}}$	13.67	F_{234}	−54.4	F_{1466}	−189.
$F_{16}=^2J_{t\beta}^{\mathrm{HH}}$	11.96	F_{245}	114.71	F_{2222}	−35.6
$F_{23}=^2J_{rs}^{\mathrm{HH}}$	−20.72	F_{255}	2.89	F_{2224}	−33.7
$F_{33}=\frac{1}{2}{}^2J_{rr}^{\mathrm{HH}}$	−18.622	F_{333}	−41.75	F_{2225}	15.1
$F_{34}=^2J_{r\alpha}^{\mathrm{HH}}$	13.66	F_{444}	−23.09	F_{2233}	−49.9
$F_{35}=^2J_{r\beta}^{\mathrm{HH}}$	15.28	F_{445}	15.85	F_{2244}	300.2
$F_{36}=^2J_{r\gamma}^{\mathrm{HH}}$	6.286	F_{456}	57.77	F_{2255}	8.2
$F_{44}=\frac{1}{2}{}^2J_{\alpha\alpha}^{\mathrm{HH}}$	30.318	F_{466}	22.10	F_{2333}	−47.7
$F_{46}=^2J_{\alpha\beta}^{\mathrm{HH}}$	18.484	F_{555}	−0.729	F_{2334}	166.
$F_{55}=\frac{1}{2}{}^2J_{\beta\beta}^{\mathrm{HH}}$	1.524	F_{556}	10.88	F_{2344}	312.
$F_{56}=^2J_{\beta\gamma}^{\mathrm{HH}}$	23.217			F_{2444}	364.9
		F_{1111}	−7.2	F_{4444}	61.76
F_{111}	−0.88	F_{1112}	−6.1	F_{4445}	9.36
F_{112}	−8.54	F_{1114}	−25.2	F_{4456}	26.1
F_{114}	0.87	F_{1122}	−9.9	F_{4466}	29.0
F_{115}	2.46	F_{1124}	−71.	F_{4555}	1.39
F_{123}	−18.6	F_{1126}	60.	F_{4556}	−2.2
F_{124}	28.8	F_{1146}	642.	F_{5566}	17.8
F_{133}	−5.81	F_{1155}	−323.9	F_{5666}	6.46
F_{135}	−17.4	F_{1156}	−624.	F_{6666}	2.62

$$\langle P\rangle_T = \mathrm{tr}(\rho_{i,i}\langle P\rangle_i), \tag{17}$$

involving the (diagonal) density matrix

$$\rho_{i,i} \equiv \frac{1}{Q}\exp\left(-\frac{E_{\mathrm{rv}}^{(i)}}{kT}\right) = \frac{1}{Q}\langle\Phi_{\mathrm{rv}}^{(i)}|\exp(-\beta H_{\mathrm{rv}})|\Phi_{\mathrm{rv}}^{(i)}\rangle \tag{18}$$

and the operator P, both given in the representation of the eigenfunctions $\Phi_{\mathrm{rv}}^{(i)}$ of the rotation-vibrational Hamiltonian H_{rv}. In Eq. (18), we introduced the standard notation $\beta = 1/kT$. Since the trace does not depend on the choice of the representation, we can evaluate Eq. (18) in any representation we find suitable. The obvious choice is to work with the representation of the *basis* functions, which in TROVE are given by

$$|\phi_{\mathrm{rv}}^{(i)}\rangle = |jkm\rangle|V\rangle, \tag{19}$$

where $|jkm\rangle$ is a symmetry-adapted rotational basis function, $|V\rangle = |n_1\rangle|n_2\rangle|n_3\rangle|n_4\rangle|n_5\rangle|n_6\rangle$ (see Ref. 68) is a short-hand notation for a vibrational basis function, and i is a short-hand index numbering the basis states.

TABLE V. The molecular symmetry groups, irreducible representations Γ, and the nuclear statistical weights g_{ns} for $^{15}NH_3$, $^{15}ND_3$, $^{15}NH_2D$, and $^{15}NDH_2$.

Molecule	Symmetry	g_{ns}					
Γ		A_1'	A_2'	E'	A_1''	A_2''	E''
$^{15}NH_3$	D_{3h}	0	8	4	0	8	4
$^{15}ND_3$	D_{3h}	20	2	16	20	2	16
Γ		A_1	A_2	B_1	B_2		
$^{15}NH_2D$	C_{2v}	6	6	18	18		
$^{15}NHD_2$	C_{2v}	24	24	12	12		

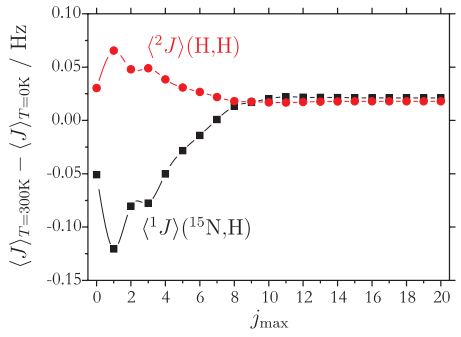

FIG. 1. Convergence of the thermally averaged N–H (squares) and H–H (circles) spin-spin coupling constants vs j_{max} plotted relative to the corresponding $T=0$ K values.

The (nondiagonal) density matrix $\rho_{l,l'}$ is constructed by expanding the matrix exponential as a Taylor series,[70]

$$\rho_{l,l'} = \frac{1}{Q}\langle\phi_{rv}^{(l)}|\exp(-\beta H_{rv})|\phi_{rv}^{(l')}\rangle = \frac{1}{Q}\sum_{k\geq 0}\frac{1}{k!}\langle\phi_{rv}^{(l)}|(-\beta H_{rv})^k|\phi_{rv}^{(l')}\rangle, \quad (20)$$

in the representation of the basis functions in Eq. (19). Thus the problem of the diagonalization of the Hamiltonian matrix $\langle\phi_{rv}^{(l)}|H_{rv}|\phi_{rv}^{(l')}\rangle$ is replaced by the problem of evaluating the matrix products in Eq. (20). In these expansions, we employed the scaling and squaring technique[70] in order to improve the convergence of the Taylor series. Usually five to ten terms in the expansion were sufficient to guarantee convergence of the average values to about 0.001 Hz. The resulting density matrix $\rho_{l,l'}$ is then utilized for averaging the spin-spin constants ^1J (^{15}N,H) and ^2J(H,H) in analogy to Eq. (17). The required matrix elements $\langle\phi_{rv}^{(l)}|P|\phi_{rv}^{(l')}\rangle$ depend solely on the vibrational coordinates and can be written as

$$\langle\phi_{rv}^{(l)}|P|\phi_{rv}^{(l')}\rangle = \langle V|P|V'\rangle\langle jkm|jk'm\rangle, \quad (21)$$

where $\langle jkm|jk'm\rangle = \delta_{k,k'}$. The integrals $\langle V|P|V'\rangle$ are computed by the technique described in Ref. 101. Before processing Eq. (20), the matrix elements $\langle\phi_{rv}^{(l)}|H_{rv}|\phi_{rv}^{(l')}\rangle$ are transformed into a symmetry adapted representation[102] to reduce the size of the matrices. The pyramidal molecules $^{15}NH_3$ and $^{15}ND_3$ are treated in the D_{3h} (M) molecular symmetry group, while C_{2v} (M) symmetry is employed for $^{15}NH_2D$ and $^{15}NDH_2$.[102] In the case of $^{15}NH_3$, the use of symmetry is especially beneficial since the A_1' and A_1'' representations have zero nuclear weight factors and do not enter into Eq. (20). The statistical weights for the relevant states were determined following the approach of Ref. 103. They are given in Table V for easy reference. The averages could be computed for each value of the rotational quantum number (the standard notation for this quantum number is J but we denote it by j here to distinguish it from the spin-spin coupling constants) j and for each irreducible representation of the molecular symmetry group independently. The maximum value of the rotational quantum number j taken into account is different for different molecules. To ensure convergence to better than 0.001 Hz, we used $j_{max}=19$, 26, 22, and 24 for $^{15}NH_3$, $^{15}ND_3$, $^{15}NH_2D$, and $^{15}NDH_2$, respectively. For the case of $^{15}NH_3$, the convergence with regard to j_{max} is illustrated in Fig. 1.

The partition function values [see Eq. (15)] were also computed using the matrix exponential technique in conjunction with the statistical weight factors from Table V. For $T=300$ K, we obtained $Q=1175.9$, 11 064.8, 7732.1, and 16 290.3 for $^{15}NH_3$, $^{15}ND_3$, $^{15}NH_2D$, and $^{15}NDH_2$, respectively.

The results of the thermal averaging ($T=300$ K) for $^{15}NH_3$ and its deuterated isotopologues are listed in Table VI. The values in parentheses are the vibrational corrections ΔJ, defined as

$$\Delta J = \langle J\rangle - J_{eq}. \quad (22)$$

Here and in the following, we report the three couplings to deuterium in terms of $^1J^*$ (^{15}N,D), $^2J^*$(H,D), and $^2J^*$(D,D), defined as

$$^1J^*(^{15}\text{N,D}) = \frac{\gamma_H}{\gamma_D}{}^1J(^{15}\text{N,D}), \quad (23)$$

TABLE VI. Calculated thermally averaged nitrogen-hydrogen and hydrogen-hydrogen spin-spin coupling constants of ammonia isotopologues. Values in parentheses are the corresponding vibrational (for $T=0$ K) and thermal (for $T=0$ K) corrections. All values are in Hz. The vibrational basis set is defined by $P\leq 10$ (see text).

	$^{15}NH_3$				$^{15}NH_2D$			
	$T=0$ K [a]		$T=300$ K		$T=0$ K		$T=300$ K	
$\langle^1J(^{15}\text{N,H})\rangle$	−61.968	(0.341)	−61.947	(0.361)	−61.923	(0.386)	−61.884	(0.425)
$\langle^1J^*(^{15}\text{N,D})\rangle$					−62.354	(−0.045)	−62.284	(0.025)
$\langle^2J(\text{H,H})\rangle$	−10.699	(0.537)	−10.681	(0.555)	−10.682	(0.554)	−10.671	(0.565)
$\langle^2J^*(\text{H,D})\rangle$					−10.732	(0.504)	−10.734	(0.502)
	$^{15}NHD_2$				$^{15}ND_3$			
	$T=0$ K		$T=300$ K		$T=0$ K		$T=300$ K	
$\langle^1J(^{15}\text{N,H})\rangle$	−61.785	(0.524)	−61.823	(0.486)				
$\langle^1J^*(^{15}\text{N,D})\rangle$	−62.205	(0.104)	−62.216	(0.093)	−62.024	(0.285)	−62.083	(0.226)
$\langle^2J^*(\text{H,D})\rangle$	−10.758	(0.478)	−10.721	(0.515)				
$\langle^2J^*(\text{D,D})\rangle$	−10.825	(0.411)	−10.795	(0.441)	−10.864	(0.372)	−10.806	(0.430)

[a]Zero-point vibrational correction for $T=0$ K have been calculated for the lowest vibrational state 0^-.

$$^2J^*(H,D) = \frac{\gamma_H}{\gamma_D} {}^2J(\mathrm{H,D}), \tag{24}$$

$$^2J^*(D,D) = \left(\frac{\gamma_H}{\gamma_D}\right)^2 {}^2J(\mathrm{D,D}), \tag{25}$$

with γ_H and γ_D being the magnetogyric ratios of hydrogen and deuterium, respectively, in order to render them comparable with the corresponding couplings to hydrogen. Table VI also contains the vibrational averages of $^{1,2}J$ at $T=0$ K, calculated as expectation values for the lowest rovibrational state (i.e., the zero-point vibrational corrections). In the case of $^{15}NH_3$, the lowest rovibrational state, i.e., the only one populated at $T=0$ K, is 0^- since its symmetric counterpart 0^+ has a statistical weight factor of zero and thus does not exist according to the Pauli principle. For comparison, we have also generated the analogous values for the (nonexisting) 0^+ state, which are $\langle 0^+|{}^1J^{\mathrm{NH}}|0^+\rangle = -62.047$ Hz and $\langle 0^+|{}^2J^{\mathrm{HH}}|0^+\rangle = -10.661$ Hz.

Upon inspection of Table VI, we note first that the vibrational corrections are generally positive both for the one-bond and the geminal couplings, i.e., vibrational averaging reduces the absolute values of both coupling constants; the only exception is the one-bond N–D coupling of NH_2D at $T=0$ K with a tiny negative correction (−0.045 Hz). Second, the total thermal averaging correction obtained from Eq. (14) is rather small for the one-bond N–H coupling in $^{15}NH_3$, 0.36 Hz or 0.6%, but more significant for the geminal proton-proton coupling, 0.55 Hz or 5.2%. This is consistent with the expansion parameters from Tables I and II, which indicate that the dominant vibrational contributions to the one-bond and geminal couplings involve the rather rigid N–H and the more flexible H–N–H deformations, respectively.

The differences between the $T=0$ K and $T=300$ K $\langle J\rangle$ values (see Table VI) suggest that the temperature dependence is negligible for both couplings. This is analyzed in more detail below.

B. Contributions to the averaged coupling constants

In previous work,[42,43,45,49,104,105] we used an alternative approach to compute the coupling constants, which is in principle applicable to all molecules. We expanded the coupling surfaces in a Taylor series to second order in internal coordinates and then calculated the vibrationally and thermally averaged coupling constants $\langle J\rangle$ by averaging over the changes in the internal coordinates. For ammonia, this treatment yields

$$\begin{aligned}\langle {}^1J(^{15}N,\mathrm{H}_1)\rangle = {}& {}^1J_0^{\mathrm{NH}} + {}^1J_r^{\mathrm{NH}}\langle\Delta r_1\rangle + {}^1J_s^{\mathrm{NH}}(\langle\Delta r_2\rangle + \langle\Delta r_3\rangle) + {}^1J_\alpha^{\mathrm{NH}}(\langle\Delta\alpha_{12}\rangle + \langle\Delta\alpha_{13}\rangle) + {}^1J_\gamma^{\mathrm{NH}}\langle\Delta\alpha_{23}\rangle + \tfrac{1}{2}{}^1J_{rr}^{\mathrm{NH}}\langle\Delta r_1^2\rangle + \tfrac{1}{2}{}^1J_{ss}^{\mathrm{NH}}(\langle\Delta r_2^2\rangle \\ & + \langle\Delta r_3^2\rangle) + \tfrac{1}{2}{}^1J_{\alpha\alpha}^{\mathrm{NH}}(\langle\Delta\alpha_{12}^2\rangle + \langle\Delta\alpha_{13}^2\rangle) + \tfrac{1}{2}{}^1J_{\gamma\gamma}^{\mathrm{NH}}\langle\Delta\alpha_{23}^2\rangle + {}^1J_{rs}^{\mathrm{NH}}(\langle\Delta r_1\Delta r_2\rangle + \langle\Delta r_1\Delta r_3\rangle) + {}^1J_{st}^{\mathrm{NH}}\langle\Delta r_2\Delta r_3\rangle \\ & + {}^1J_{r\alpha}^{\mathrm{NH}}(\langle\Delta r_1\Delta\alpha_{12}\rangle + \langle\Delta r_1\Delta\alpha_{13}\rangle) + {}^1J_{r\gamma}^{\mathrm{NH}}\langle\Delta r_1\Delta\alpha_{23}\rangle + {}^1J_{s\alpha}^{\mathrm{NH}}(\langle\Delta r_2\Delta\alpha_{12}\rangle + \langle\Delta r_3\Delta\alpha_{13}\rangle) + {}^1J_{s\beta}^{\mathrm{NH}}(\langle\Delta r_2\Delta\alpha_{13}\rangle \\ & + \langle\Delta r_3\Delta\alpha_{12}\rangle) + {}^1J_{s\gamma}^{\mathrm{NH}}(\langle\Delta r_2\Delta\alpha_{23}\rangle + \langle\Delta r_3\Delta\alpha_{23}\rangle) + {}^1J_{\alpha\beta}^{\mathrm{NH}}\langle\Delta\alpha_{12}\Delta\alpha_{13}\rangle + {}^1J_{\alpha\gamma}^{\mathrm{NH}}(\langle\Delta\alpha_{12}\Delta\alpha_{23}\rangle + \langle\Delta\alpha_{13}\Delta\alpha_{23}\rangle),\end{aligned} \tag{26}$$

$$\begin{aligned}\langle {}^2J(\mathrm{H}_2,\mathrm{H}_3)\rangle = {}& {}^2J_0^{\mathrm{HH}} + {}^2J_r^{\mathrm{HH}}(\langle\Delta r_2\rangle + \langle\Delta r_3\rangle) + {}^2J_t^{\mathrm{HH}}\langle\Delta r_1\rangle + {}^2J_\alpha^{\mathrm{HH}}\langle\Delta\alpha_{23}\rangle + {}^2J_\beta^{\mathrm{HH}}(\langle\Delta\alpha_{12}\rangle + \langle\Delta\alpha_{13}\rangle) + \tfrac{1}{2}{}^2J_{rr}^{\mathrm{HH}}(\langle\Delta r_2^2\rangle + \langle\Delta r_3^2\rangle) \\ & + \tfrac{1}{2}{}^2J_{tt}^{\mathrm{HH}}\langle\Delta r_1^2\rangle + \tfrac{1}{2}{}^2J_{\alpha\alpha}^{\mathrm{HH}}\langle\Delta\alpha_{23}^2\rangle + \tfrac{1}{2}{}^2J_{\beta\beta}^{\mathrm{HH}}(\langle\Delta\alpha_{12}^2\rangle + \langle\Delta\alpha_{13}^2\rangle) + {}^2J_{rs}^{\mathrm{HH}}\langle\Delta r_2\Delta r_3\rangle + {}^2J_{rt}^{\mathrm{HH}}(\langle\Delta r_1\Delta r_2\rangle + \langle\Delta r_1\Delta r_3\rangle) \\ & + {}^2J_{r\alpha}^{\mathrm{HH}}(\langle\Delta r_2\Delta\alpha_{23}\rangle + \langle\Delta r_3\Delta\alpha_{23}\rangle) + {}^2J_{r\beta}^{\mathrm{HH}}(\langle\Delta r_2\Delta\alpha_{12}\rangle + \langle\Delta r_3\Delta\alpha_{13}\rangle) + {}^2J_{t\alpha}^{\mathrm{HH}}\langle\Delta r_1\Delta\alpha_{23}\rangle + {}^2J_{t\beta}^{\mathrm{HH}}(\langle\Delta r_1\Delta\alpha_{12}\rangle \\ & + \langle\Delta r_1\Delta\alpha_{13}\rangle) + {}^2J_{r\gamma}^{\mathrm{HH}}(\langle\Delta r_2\Delta\alpha_{13}\rangle + \langle\Delta r_3\Delta\alpha_{12}\rangle) + {}^2J_{\alpha\beta}^{\mathrm{HH}}(\langle\Delta\alpha_{12}\Delta\alpha_{23}\rangle + \langle\Delta\alpha_{13}\Delta\alpha_{23}\rangle) + {}^2J_{\beta\gamma}^{\mathrm{HH}}\langle\Delta\alpha_{12}\Delta\alpha_{13}\rangle.\end{aligned} \tag{27}$$

The expansion coefficients, $J_r, J_\alpha, \ldots$ in Eqs. (26) and (27) are almost identical to the F coefficients in Eq. (7) as seen from in Tables III and IV. In our previous work,[42,43,45,104,105] we then used first- and second-order perturbation theory to calculate average normal-coordinate displacements which were subsequently transformed to average internal-coordinate displacements, $\langle\Delta r_1\rangle$, $\langle\Delta\alpha_{23}\rangle, \ldots$. In the present work, we can obtain these average internal-coordinate displacements directly from the density matrix as given in Eqs. (17) and (18).

The mean geometrical parameters entering into Eqs. (26) and (27) for $^{15}NH_3$ and $^{15}ND_3$ are collected in Table VII. They can be utilized for averaging arbitrary properties of $^{15}NH_3$ and $^{15}ND_3$ as long as these can be represented as second-order Taylor expansions similar to Eqs. (26) and (27).

In Table VIII, we present the averaged values of the spin-spin constants $\langle J\rangle$ for $^{15}NH_3$ and $^{15}ND_3$ obtained via the second-order Taylor expansion, Eqs. (26) and (27). Compared with the full treatment, the second-order expansion only slightly overestimates the vibrational corrections to the one-bond coupling, by 0.05 Hz ($T=300$ K) for $^{15}NH_3$ and by even less for $^{15}ND_3$, while the differences are negligible for the geminal H–H or D–D couplings. The second-order treatment represented by the expansions (26) and (27) thus appears to be sufficient, at least for moderate temperatures. This might seem unexpected for a molecule such as ammo-

TABLE VII. Mean geometrical parameters of two ammonia isotopologues at 0 and 300 K compared with $H_2{}^{16}O$ (taken from Ref. 104). Bond lengths in Å and bond angles in rad.

	$^{15}NH_3$		$^{15}ND_3$		$H_2{}^{16}O$ [a]
Geometrical parameter	0 K[b]	300 K	0 K[b]	300 K	300 K
$\langle\Delta r_1\rangle$	0.019 313	0.019 945	0.014 077	0.014 768	0.017 75
$\langle\Delta r_1^2\rangle$	0.005 597	0.005 631	0.003 973	0.004 004	0.004 60
$\langle\Delta r_1\Delta r_2\rangle$	0.000 369	0.000 395	0.000 168	0.000 191	0.000 02
$\langle\Delta\alpha_{23}\rangle$	−0.000 329	−0.000 396	−0.000 938	−0.000 501	−0.004 17
$\langle\Delta\alpha_{23}^2\rangle$	0.024 070	0.024 239	0.017 739	0.018 123	0.023 89
$\langle\Delta\alpha_{23}\Delta\alpha_{13}\rangle$	−0.001 151	−0.000 953	−0.000 574	−0.000 272	
$\langle\Delta r_1\Delta\alpha_{23}\rangle$	0.000 039	0.000 022	0.000 108	0.000 071	
$\langle\Delta r_1\Delta\alpha_{13}\rangle$	−0.000 812	−0.000 831	−0.000 741	−0.000 747	−0.000 81

[a]Reference 104.
[b]Computed for the 0^- eigenstate (see text).

nia, which is known to be very anharmonic. However, one has to remember that our approach to the thermal averaging explicitly takes into account the nonrigid character of the flexible umbrella mode and correctly describes the tunneling through the low inversion barrier of ammonia. This is achieved through an appropriate construction of the basis functions $|V\rangle$ in Eq. (19). In order to demonstrate the importance of this point for the description of $\langle J\rangle$, we have recomputed the averages of the coupling constants for $^{15}NH_3$ by employing a rigid-molecule approach, i.e., by treating ammonia as a rigid C_{3v} system, with the potential function expanded up to the fourth order and the kinetic energy operator up to the second order. This should mimic the standard anharmonic approach that is commonly utilized for vibrational averaging.[29,37,42,43,45,47,49–54] Even though this rigid-molecule approach does not employ perturbation theory to generate the vibrational wave functions and our basis does not consist of the usual harmonic-oscillator functions, the analogy with the second-order perturbation treatment is close, as our internal (linearized) coordinates (see Ref. 68) are connected with the normal coordinates through a linear transformation. The computed "rigid" values of $\langle J\rangle$, −62.155 and −10.556 Hz for the nitrogen-proton and geminal H–H coupling constants, respectively, deviate substantially both from the nonrigid values (see Table VI) and from the values obtained using Eqs. (26) and (27). The vibrational correction to the geminal coupling (0.680 Hz) is significantly overestimated, while the correction to the one-bond coupling (0.154 Hz) is too small. These values can be much improved by introducing more terms into the expansions of the potential energy function (still treated as a single minimum) and the kinetic energy operator. For example, extending these up to the eighth and sixth order, respectively, we obtain $\langle {}^1J(^{15}\mathrm{N},\mathrm{H}_1)\rangle = -61.891$ Hz and $\langle {}^2J(\mathrm{H}_2,\mathrm{H}_3)\rangle = -10.712$ Hz, i.e., much closer to the nonrigid values. The remaining discrepancy (0.056 and −0.031 Hz, respectively) can then be attributed to the single-well character of the rigid approach.

The reasonably good agreement between the results from the second-order treatment and from the proper thermal averaging with the use of TROVE variational wave functions allows us to follow previous studies on methane, water, ethylene, and silane[42,43,45,47,49] and to analyze the thermal corrections in terms of contributions from the individual internal coordinates (Table IX). For the one-bond coupling, we find first-order and second-order stretch contributions of 1.236 and 0.626 Hz, respectively, whose sum (1.862 Hz) is almost completely canceled by the negative second-order bend contribution of −1.588 Hz. For the geminal coupling, the second-order bend contribution of 0.751 Hz is dominant and only slightly reduced by the second-order stretch contribution ${}^2J_{rs}^{\mathrm{HH}} = -0.213$ Hz. In the rigid approach, it is mostly the bending linear contributions that are responsible for the deviations from the nonrigid results since the absolute values of

TABLE VIII. Comparison of the thermally averaged nitrogen-hydrogen and hydrogen-hydrogen spin-spin coupling constants of ammonia isotopologues calculated using the second-order Taylor expansions, see Eqs. (26) and (27). Values in parenthesis are the corresponding vibrational (for $T=0$ K) and thermal (for $T=300$ K) corrections. All values are in Hz.

Temperature (K)	$^{15}NH_3$ [a]				$^{15}ND_3$			
	$^1J(^{15}\mathrm{N},\mathrm{H})$		$^2J(\mathrm{H},\mathrm{H})$		$^1J^*(^{15}\mathrm{N},\mathrm{D})$		$^2J^*(\mathrm{D},\mathrm{D})$.	
	Based on nonrigid molecule							
0	−61.936	(0.374)	−10.692	(0.544)	−62.013	(0.297)	−10.855	(0.381)
300	−61.900	(0.409)	−10.671	(0.565)	−62.056	(0.254)	−10.802	(0.434)
	Based on (4–2) rigid C_{3v} molecule							
300	−62.155	(0.154)	−10.556	(0.680)				
	Based on (8–6) rigid C_{3v} molecule							
300	−61.891	(0.418)	−10.712	(0.524)				

[a]Zero-point vibrational correction (T=0 K) have been calculated for the lowest A_2'' vibrational state.

TABLE IX. Nuclear motion contributions to the total nitrogen-hydrogen and hydrogen-hydrogen spin-spin coupling constants of $^{15}NH_3$ at 300 and 600 K of terms involving the individual internal coordinate and the inversion mode coefficients, Eqs. (26) and (27) computed using the full nonrigid and the simplest rigid approach (see text). All values are in Hz.

	^1J (^{15}N,H)			^2J(H,H)			
	300 K		600 K		300 K		600 K
	Nonrigid	Rigid	Nonrigid		Nonrigid	Rigid	Nonrigid
$^1J_r^{NH}$	1.620	1.600	1.665	$^2J_t^{HH}$	0.078	0.077	0.080
$^1J_s^{NH}$	−0.384	−0.380	−0.395	$^2J_r^{HH}$	0.034	0.034	0.035
First order stretch	1.236	1.220	1.270		0.113	0.111	0.116
$^1J_{rr}^{NH}$	0.229	0.227	0.230	$^2J_{tt}^{HH}$	0.000	0.000	0.000
$^1J_{rs}^{NH}$	0.035	0.034	0.038	$^2J_{rr}^{HH}$	0.006	0.005	0.006
$^1J_{st}^{NH}$	0.004	0.004	0.005	$^2J_{rt}^{HH}$	−0.008	−0.008	−0.009
$^1J_{ss}^{NH}$	0.359	0.356	0.362	$^2J_{rs}^{HH}$	−0.210	−0.208	−0.211
Second order stretch	0.626	0.622	0.634		−0.213	−0.211	−0.215
Total stretch to 2nd order	1.862	1.842	1.904		−0.100	−0.100	−0.099
$^1J_\gamma^{NH}$	0.004	−0.015	−0.032	$^2J_\alpha^{HH}$	−0.019	0.073	0.162
$^1J_\alpha^{NH}$	0.036	−0.138	−0.304	$^2J_\beta^{HH}$	0.000	−0.001	−0.003
First order bend	0.040	−0.153	−0.336		−0.019	0.072	0.159
$^1J_{\gamma\gamma}^{NH}$	−0.167	−0.169	−0.184	$^2J_{\alpha\alpha}^{HH}$	0.735	0.745	0.809
$^1J_{\alpha\alpha}^{NH}$	−1.500	−1.521	−1.652	$^2J_{\beta\beta}^{HH}$	0.074	0.075	0.081
$^1J_{\alpha\gamma}^{NH}$	0.047	0.041	−0.015	$^2J_{\alpha\beta}^{HH}$	−0.035	−0.031	0.011
$^1J_{\alpha\beta}^{NH}$	0.032	0.027	−0.010	$^2J_{\beta\gamma}^{HH}$	−0.022	−0.019	0.007
Second order bend	−1.588	−1.622	−1.861		0.751	0.771	0.910
Total bend to second order	−1.548	−1.775	−2.197		0.733	0.843	1.068
$^1J_{r\gamma}^{NH}$	−0.001	−0.003	0.001	$^2J_{t\alpha}^{HH}$	0.000	0.001	0.000
$^1J_{r\alpha}^{NH}$	0.102	0.097	0.110	$^2J_{t\beta}^{HH}$	−0.020	−0.019	−0.021
$^1J_{s\gamma}^{NH}$	0.037	0.035	0.040	$^2J_{r\alpha}^{HH}$	−0.023	−0.022	−0.025
$^1J_{s\alpha}^{NH}$	−0.043	−0.041	−0.046	$^2J_{r\beta}^{HH}$	−0.025	−0.024	−0.027
$^1J_{s\beta}^{NH}$	−0.001	−0.002	0.000	$^2J_{r\gamma}^{HH}$	0.000	0.001	0.000
Second order stretch-bend	0.095	0.087	0.105		−0.067	−0.063	−0.074
Total correction to secod order	0.409	0.154	−0.188		0.565	0.680	0.895
Third and fourth orders			−0.113				0.033

$^1J_\alpha^{NH}$ and $^2J_\alpha^{HH}$ are overestimated by 0.17 and 0.09 Hz, respectively.

For the sake of comparison, we have also included in Table VII the values of the mean geometrical parameters for water,[104] which were obtained using perturbation theory. It is somewhat surprising that the mean changes in the geometrical parameters are almost the same in NH_3 and H_2O. An analysis of the computed spin-spin coupling constants of water in terms of internal coordinates[43] also concluded that the zero-point vibrational corrections reduce the absolute values of the one-bond O–H and the geminal H–H coupling constants. Compared with ammonia, the zero-point vibrational corrections for the one-bond coupling are more pronounced in water (7.6% versus 4.9%) due to the fact that the first-order stretch contribution is about three times larger and the second-order bend contribution is about half as large.

C. Rotation-vibration interaction

When averaging molecular properties, the effects of rotation-vibration interactions are commonly disregarded. Sometimes rotational effects are entirely neglected in that the required energies, matrix elements, and partition functions are constructed from vibrational contributions only. Sometimes it is assumed that in Eq. (14), $E_{rv}^{(i)}=E_{vib}^{(i)}+E_{rot}^{(i)}$ and, correspondingly, $Q=Q_{vib}Q_{rot}$, where the rotational energies $E_{rot}^{(i)}$ are taken to be those for the vibrational ground state. In the present treatment, we calculate $E_{rv}^{(i)}$ and Q using "fully coupled" rotation-vibration wave functions, and thus we take into account all rotation-vibration interactions such as Coriolis effects. This allows us to investigate the importance of the rotation-vibration coupling effects for thermal averaging and thus assess the accuracy of the pure vibrational averaging approach in which rotation is ignored. In our approach, vibrational averaging corresponds to $\langle J\rangle$ values computed from the vibrational ($j=0$) wave functions only. The resulting values of $\langle J\rangle$ will be referred to as $\langle J\rangle_{j=0}$. For $^{15}NH_3$ we obtain $\langle {}^1J\rangle_{j=0}=-62.019$ Hz and $\langle {}^2J\rangle_{j=0}=-10.669$ Hz at 300 K. These values differ from the $T=0$ K values $\langle J\rangle_{T=0\ K}$, which are also obtained from pure vibrational integrations, the deviations (−0.051 and 0.030 Hz, respectively) reflecting the temperature dependence of the purely vibrational averages. Interestingly, these differences are significantly larger than those resulting from "complete" thermal averaging with all relevant j values included, which are obtained from the $\langle J\rangle_{T=300\ K}$ and $\langle J\rangle_{T=0\ K}$ values (see Table VI). In Fig. 1 we demonstrate that the rotational contributions (from $j>0$) are almost as large as the vibrational ones, but with opposite

sign; hence, there is significant cancellation, and small thermal corrections ensue. Figure 1 depicts thermal corrections $\Delta J_{T=300\ \mathrm{K}}$ defined as

$$\Delta J_{T=300\ \mathrm{K}} = \langle J \rangle_{T=300\ \mathrm{K}} - \langle J \rangle_{T=0\ \mathrm{K}} \tag{28}$$

and computed for different values of the maximal rotational quantum number $j_{\max}$. As j increases, there is first a rather large oscillation at $j=1$ and then the total thermal correction converges to 0.021 Hz ($\langle {}^1J \rangle_{T=300\ \mathrm{K}}$) and 0.018 Hz ($\langle {}^2J \rangle_{T=300\ \mathrm{K}}$). For the rotational correction (i.e., the contributions from $j>0$ states), we obtain 0.072 and −0.012 Hz, respectively. These values are too large to be ignored. Thus the final thermal correction is small, but only when it is properly evaluated.

D. Higher temperatures

In order to gain a better understanding of the temperature effects, we have performed thermal averaging of ${}^1J$ (^{15}N,H) and ${}^2J$(H,H) for ${}^{15}NH_3$ also at $T=600$ K, obtaining averages of −62.610 and −10.308 Hz, respectively. At $T=600$ K, we had to use $j_{\max}=30$ to reach convergence, with the partition function for ${}^{15}NH_3$ being $Q=3851.8$. The contributions to the vibrational corrections for the spin-spin coupling constants are collected in Table IX so that they can be compared with the $T=300$ K values. In contrast to the $T=300$ K results, where the bending and stretching contributions in Eqs. (26) and (27) partially cancel each other, the bending contributions exceed the stretching ones at $T=600$ K, resulting in a significant negative correction (−0.301 Hz) for the one-bond coupling and in a large positive correction (0.928 Hz) for the geminal coupling relative to the corresponding $T=0$ K values. The effect from higher (third and fourth) order terms in the Hamiltonian at $T=600$ K is now notable for the one-bond coupling (−0.113 Hz) but still rather small for the geminal coupling (0.033 Hz). The rotational effects (i.e., contributions from states with $j>0$) are less important at $T=600$ K, namely −0.056 Hz for the one-bond coupling (relative to ${}^1J_{j_{\max}=0}=-62.554$ Hz) and 0.074 Hz for the geminal coupling (relative to ${}^2J_{j_{\max}=0}=-10.382$ Hz). This is to be expected. As far as thermal averaging is concerned, the rotation at high temperature can be safely separated from the vibration, which effectively removes the rotational contributions. The vibrational thermal effect ($j=0$) is quite large at $T=600$ K for both coupling constants, with $\Delta\,{}^1J_{T=600\ \mathrm{K}}=-0.586$ Hz and $\Delta\,{}^2J_{T=600\ \mathrm{K}}=0.317$ Hz as follows from Eq. (28).

E. Comparison with experiment and earlier calculations

In Table X, we compare our present results for vibrationally averaged spin-spin coupling constants in ammonia with those from earlier calculations. We note that only the very recent DFT/B3LYP calculation by Ruden *et al.*[53] gives results comparable to ours. In two early studies,[66,67] the values for the vibrational ground states are far off the experimental values. This must be due to an insufficient basis set and/or level of correlation in these calculations. The recent DFT study[53] leads to averaged coupling constants close to our values; however, the vibrational corrections obtained by second-order perturbation theory are too large compared to our variational treatment. Our second-order rigid molecule treatment reproduces the reported correction for the two-bond hydrogen-hydrogen coupling[53] rather well, but the reported correction to the one-bond coupling remains too large even if we account for the rotational effect (about 0.07 Hz, see Fig. 1 and discussion above).

TABLE X. Results of previous calculations of the nitrogen-proton coupling, ${}^1J$ (^{15}N,H), and proton-proton coupling, ${}^2J$(H,H), in the vibrational ground state of ammonia ${}^{15}NH_3$. All values are in Hz and are presented in order of the date of publication.

Method	Ref.	${}^1J$ (${}^{14/15}$N,H)	${}^2J$(H,H)
CISD[a]	66	···	−8.28
INDO[b]	67	−37.39	−9.29
INDO[c]	67	−40.34	−8.57
DFT/B3LYP[d]	53	−63.7	−9.4
SOPPA(CCSD)	This work	−61.97	−10.70

[a]Basis set: N: (9s5p1d)→[4s2p1d], H: (5s1p)→[3s1p]; vibrational averaging over the two symmetric normal modes (symmetric stretch and inversion mode) using variationally determined linear combinations of products of harmonic oscillator wave functions.
[b]Vibrational averaging over all six normal modes using perturbation theory with only zeroth order vibrational wave functions, i.e., products of harmonic oscillator functions. No contribution from the anharmonicity of the potential or the coupling of normal modes.
[c]Vibrational averaging over the inversion mode with a numerical wave function and over the other normal modes with the vibrational wave function as product of harmonic oscillator functions, i.e., no contribution from the anharmonicity of the potential other than in the inversion mode or the coupling of normal modes.
[d]Basis set: HuzIII-su3; vibrational averaging over all six normal modes using perturbation theory to second order and zeroth and first order vibrational wave functions—contribution from the anharmonicity of the potential included.

Finally, in Table XI, we have collected the available experimental values of the one- and two-bond coupling constants in different isotopologues of ammonia. A complete set of data was presented by Wasylishen and Friedrich[109] who also produced the values with the smallest error bars up to date. Unfortunately their measurements were carried out in the liquid phase and not in a vapor as e.g., in the old study by Alei *et al.*,[108] so that their data are not directly comparable to our theoretical gas-phase values. However, we can correct the measured ${}^1J$ (^{15}N,H) coupling constant in ${}^{15}NH_3$ with the vapor-to-liquid shift recently calculated at the B3LYP level by Gester *et al.*[71] This leads to an empirical gas phase value of −61.95 Hz for ${}^1J$ (^{15}N,H) in ${}^{15}NH_3$ which is in excellent agreement with our thermally averaged value of −61.97 Hz.

Furthermore we can compare with the measured isotope shifts. Experimentally the primary isotope shift for the one-bond coupling is -0.46 ± 0.13 Hz, while the secondary isotope shift is 0.07 ± 0.02 Hz.[109] Our theoretical values are −0.33 Hz for the primary and 0.06–0.07 Hz for the secondary isotope effects in ${}^{15}NH_2D$ and ${}^{15}NHD_2$, again in very good agreement with experiment. Slight deviations from experiment are encountered for the isotope effects in ${}^{15}ND_3$ and for the secondary isotope effects on the H–D geminal couplings (where our values are too small). However, one

TABLE XI. Experimental values of the nitrogen-proton coupling, ^1J (^{15}N,H), or nitrogen-deuterium coupling, $^1J^*(^{15}\mathrm{N,D})=(\gamma_H/\gamma_D)^1J(^{15}\mathrm{N,D})$, and proton-deuterium coupling, $^2J^*(\mathrm{H,D})=(\gamma_H/\gamma_D)^2J(\mathrm{H,D})$. All values are in Hz and are presented in order of the date of publication.

Coupling	Phase	Ref.	$^{15}NH_3$	$^{15}NH_2$ D	$^{15}NHD_2$	$^{15}ND_3$
^1J (^{15}N,H)	Liquid	106	$\lvert 61.2 \pm 0.9 \rvert$	⋯	⋯	⋯
^1J (^{15}N,H)	Liquid (room temperature)	107	$\lvert 61.8 \pm 0.5 \rvert$	⋯	⋯	⋯
^1J (^{15}N,H)	Vapor	108	$\lvert 61.2 \pm 0.3 \rvert$	⋯	⋯	⋯
^1J (^{15}N,H)	Liquid (20 °C)	109	-61.45 ± 0.03	-61.38 ± 0.07	-61.31 ± 0.04	⋯
$^1J^*$ (^{15}N,D)	Liquid (20 °C)	109	⋯	-61.85 ± 0.04	-61.77 ± 0.06	-61.69 ± 0.01
$^2J^*$(H,D)	Liquid	106	⋯	$\lvert 10.35 \pm 0.80 \rvert$	$\lvert 10.35 \pm 0.80 \rvert$	⋯
$^2J^*$(H,D)	Liquid (20 °C)	109	⋯	-9.61 ± 0.03	-9.35 ± 0.03	⋯

should note that the solvent effect on the geminal couplings was estimated to be 2.5 Hz,[71] which is ten times larger than the isotope effect. The discrepancies between our calculated gas phase isotope shifts and the values measured in solution are therefore likely to be caused by solvent effects.

IV. SUMMARY

We have calculated point-wise surfaces of the one-bond and two-bond spin-spin coupling constants in ammonia at the level of SOPPA(CCSD) employing a specialized large one-electron basis set. Both surfaces, consisting of 2523 points each, were fitted to a fourth-order power series in the internal coordinates and subsequently thermally averaged using variational vibrational wave functions obtained from the TROVE Hamiltonian in conjunction with a CCSD(T)-based potential energy surface.

Vibrational and thermal averaging at 300 K leads to a rather small correction of 0.36 Hz or 0.6% for the one-bond nitrogen-hydrogen coupling constant in $^{15}NH_3$ and to a more notable correction of 0.56 Hz or 5.0% for the hydrogen-deuterium two-bond coupling constant in $^{15}NH_2$ D. Analyzing the contributions to the nuclear-motion corrections through second order in a Taylor expansion in internal coordinates for the nonrigid ammonia molecule, we observe that the dominant contributions to the one-bond coupling are the negative second-order bending terms $\frac{1}{2}{}^1J^{\mathrm{NH}}_{\alpha\alpha}(\langle\Delta\alpha_{12}^2\rangle + \langle\Delta\alpha_{13}^2\rangle)$ and the positive first-order own-bond stretching term $^1J_r^{\mathrm{NH}}\langle\Delta r_1\rangle$. Thus, the bending motion increases the absolute value of the one-bond coupling constant whereas the stretching motion decreases it, leading to substantial cancellation and an overall slight decrease. For the two-bond coupling, the positive second-order bending term $\frac{1}{2}{}^2J^{\mathrm{HH}}_{\alpha\alpha}\langle\Delta\alpha_{23}^2\rangle$ dominates so that the vibrational correction decreases the absolute value of the coupling constant.

Compared with our full variational treatment of nuclear motion, the standard perturbation-theory approach for a rigid ammonia molecule underestimates the nuclear motion correction to ^1J(N,H) by 57% (mainly due to the inadequate treatment of the large amplitude inversion mode), while the correction to ^2J(H,H) is overestimated (by 30%).

Comparison with the available experimental data reveals excellent agreement for the absolute values of the one-bond couplings and their primary and secondary isotope effects, while there are some slight deviations for the geminal hydrogen-deuterium couplings.

ACKNOWLEDGMENTS

S.P.A.S. acknowledges grants from the Danish Center for Scientific Computing, from the Carlsberg Foundation and from the Danish Natural Science Research Council/The Danish Councils for Independent Research (Grant No. 272-08-0486). This work was supported also by Grant No. IAA 401870702 from the Grant Agency of the Academy of Sciences of the Czech Republic.

[1] T. Helgaker, M. Jaszuński, and K. Ruud, Chem. Rev. (Washington, D.C.) **99**, 293 (1999).
[2] J. Vaara, Phys. Chem. Chem. Phys. **9**, 5399 (2007).
[3] L. B. Krivdin and R. H. Contreras, Annu. Rep. NMR Spectrosc. **61**, 133 (2007).
[4] J. M. Schulman and D. N. Kaufman, J. Chem. Phys. **57**, 2328 (1972).
[5] T. Helgaker, M. Jaszuński, K. Ruud, and A. Górska, Theor. Chem. Acc. **99**, 175 (1998).
[6] T. Enevoldsen, J. Oddershede, and S. P. A. Sauer, Theor. Chem. Acc. **100**, 275 (1998).
[7] J. Guilleme and J. San Fabián, J. Chem. Phys. **109**, 8168 (1998).
[8] P. F. Provasi, G. A. Aucar, and S. P. A. Sauer, J. Chem. Phys. **115**, 1324 (2001).
[9] J. E. Peralta, G. E. Scuseria, J. R. Cheeseman, and M. J. Frisch, Chem. Phys. Lett. **375**, 452 (2003).
[10] W. Deng, J. R. Cheeseman, and M. J. Frisch, J. Chem. Theory Comput. **2**, 1028 (2006).
[11] F. Jensen, J. Chem. Theory Comput. **2**, 1360 (2006).
[12] U. Benedikt, A. A. Auer, and F. Jensen, J. Chem. Phys. **129**, 064111 (2008).
[13] Y. Y. Rusakov, L. B. Krivdin, S. P. A. Sauer, E. P. Levanova, and G. G. Levkovskaya, Magn. Reson. Chem. **48**, 44 (2010).
[14] F. Jensen, "The optimum contraction of basis sets for calculating spin-spin coupling constants," Theor. Chim. Acta, doi:10.1007/s00214-009-0699-5 (in press).
[15] G. E. Scuseria and R. H. Contreras, Theor. Chim. Acta **59**, 437 (1981).
[16] G. E. Scuseria, A. R. Engelmann, and R. H. Contreras, Theor. Chim. Acta **61**, 49 (1982).
[17] G. E. Scuseria and R. H. Contreras, Chem. Phys. Lett. **93**, 425 (1982).
[18] G. A. Aucar and R. H. Contreras, J. Magn. Reson. **93**, 413 (1991).
[19] R. H. Contreras, M. C. Ruiz de Azúa, C. G. Giribet, G. A. Aucar, and R. Loboyan de Bonczok, J. Mol. Struct.: THEOCHEM **284**, 249 (1993).
[20] R. M. Lobayan and G. A. Aucar, J. Mol. Struct.: THEOCHEM **452**, 1 (1998).
[21] R. M. Lobayan and G. A. Aucar, J. Mol. Struct.: THEOCHEM **452**, 13 (1998).

[22] P. F. Provasi, G. A. Aucar, and S. P. A. Sauer, Int. J. Mol. Sci. **4**, 231 (2003).
[23] O. Malkina, D. R. Salahub, and V. G. Malkin, J. Chem. Phys. **105**, 8793 (1996).
[24] J. E. Peralta, V. Barone, R. H. Contreras, D. G. Zaccari, and J. P. Snyder, J. Am. Chem. Soc. **123**, 9162 (2001).
[25] P. Lantto, J. Vaara, and T. Helgaker, J. Chem. Phys. **117**, 5998 (2002).
[26] V. Barone, P. F. Provasi, J. E. Peralta, J. P. Snyder, S. P. A. Sauer, and R. H. Contreras, J. Phys. Chem. A **107**, 4748 (2003).
[27] S. P. A. Sauer, J. Phys. B **30**, 3773 (1997).
[28] J. Olsen and P. Jørgensen, J. Chem. Phys. **82**, 3235 (1985).
[29] O. Vahtras, H. Ågren, P. Jørgensen, H. J. A. Jensen, S. B. Padkjær, and T. Helgaker, J. Chem. Phys. **96**, 6120 (1992).
[30] S. A. Perera, H. Sekino, and R. J. Bartlett, J. Chem. Phys. **101**, 2186 (1994).
[31] H. Sekino and R. J. Bartlett, Chem. Phys. Lett. **225**, 486 (1994).
[32] S. A. Perera, M. Nooijen, and R. J. Bartlett, J. Chem. Phys. **104**, 3290 (1996).
[33] A. A. Auer and J. Gauss, J. Chem. Phys. **115**, 1619 (2001).
[34] J. E. Del Bene, I. Alkorta, and J. Elguero, J. Chem. Theory Comput. **4**, 967 (2008).
[35] A. A. Auer and J. Gauss, Chem. Phys. **356**, 7 (2009).
[36] J. Oddershede, J. Geertsen, and G. E. Scuseria, J. Phys. Chem. **92**, 3056 (1988).
[37] J. Geertsen, J. Oddershede, W. T. Raynes, and G. E. Scuseria, J. Magn. Reson. **93**, 458 (1991).
[38] W. T. Raynes, J. Geertsen, and J. Oddershede, Chem. Phys. Lett. **197**, 516 (1992).
[39] J. Geertsen, J. Oddershede, and W. T. Raynes, Magn. Reson. Chem. **31**, 722 (1993).
[40] W. T. Raynes, J. Geertsen, and J. Oddershede, Int. J. Quantum Chem. **52**, 153 (1994).
[41] J. Geertsen, J. Oddershede, W. T. Raynes, and T. L. Marvin, Mol. Phys. **82**, 29 (1994).
[42] R. D. Wigglesworth, W. T. Raynes, S. P. A. Sauer, and J. Oddershede, Mol. Phys. **92**, 77 (1997).
[43] R. D. Wigglesworth, W. T. Raynes, S. P. A. Sauer, and J. Oddershede, Mol. Phys. **94**, 851 (1998).
[44] S. P. A. Sauer, C. K. Møller, H. Koch, I. Paidarová, and V. Špirko, Chem. Phys. **238**, 385 (1998).
[45] R. D. Wigglesworth, W. T. Raynes, S. Kirpekar, J. Oddershede, and S. P. A. Sauer, J. Chem. Phys. **112**, 3735 (2000).
[46] S. P. A. Sauer and W. T. Raynes, J. Chem. Phys. **113**, 3121 (2000).
[47] R. D. Wigglesworth, W. T. Raynes, S. Kirpekar, J. Oddershede, and S. P. A. Sauer, J. Chem. Phys. **114**, 9192 (2001).
[48] S. P. A. Sauer and W. T. Raynes, J. Chem. Phys. **114**, 9193 (2001).
[49] S. P. A. Sauer, W. T. Raynes, and R. A. Nicholls, J. Chem. Phys. **115**, 5994 (2001).
[50] S. Kirpekar, T. Enevoldsen, J. Oddershede, and W. T. Raynes, Mol. Phys. **91**, 897 (1997).
[51] P.-O. Åstrand, K. Ruud, K. V. Mikkelsen, and T. Helgaker, J. Chem. Phys. **110**, 9463 (1999).
[52] J. Casanueva, J. San Fabián, E. Díez, and A. L. Esteban, J. Mol. Struct. **565–566**, 449 (2001).
[53] T. A. Ruden, O. B. Lutnæs, and T. Helgaker, J. Chem. Phys. **118**, 9572 (2003).
[54] T. A. Ruden, T. Helgaker, and M. Jaszuński, Chem. Phys. **296**, 53 (2004).
[55] M. B. Hansen, J. Kongsted, D. Toffoli, and O. Christiansen, J. Phys. Chem. A **112**, 8436 (2008).
[56] S. P. A. Sauer and P. F. Provasi, ChemPhysChem **9**, 1259 (2008).
[57] P. F. Provasi and S. P. A. Sauer, Phys. Chem. Chem. Phys. **11**, 3987 (2009).
[58] V. Špirko, J. Mol. Spectrosc. **101**, 30 (1983).
[59] V. Špirko and W. P. Kraemer, J. Mol. Spectrosc. **133**, 331 (1989).
[60] W. Hüttner, U. E. Frank, W. Majer, K. Mayer, and V. Špirko, Mol. Phys. **64**, 1233 (1988).
[61] V. Špirko, H. J. A. Jensen, and P. Jørgensen, Chem. Phys. **144**, 343 (1990).
[62] S. P. A. Sauer, V. Špirko, and J. Oddershede, Chem. Phys. **153**, 189 (1991).
[63] C. J. Jameson, A. C. de Dios, and A. K. Jameson, J. Chem. Phys. **95**, 1069 (1991).
[64] J. Oddershede, I. Paidarová, and V. Špirko, J. Mol. Spectrosc. **152**, 342 (1992).
[65] I. Paidarová, V. Špirko, and J. Oddershede, J. Mol. Spectrosc. **160**, 311 (1993).
[66] J. Kowalewski and B. Roos, Chem. Phys. **11**, 123 (1975).
[67] P. Solomon and J. M. Schulman, J. Am. Chem. Soc. **99**, 7776 (1977).
[68] S. N. Yurchenko, W. Thiel, and P. Jensen, J. Mol. Spectrosc. **245**, 126 (2007).
[69] S. N. Yurchenko, J. Zheng, H. Lin, P. Jensen, and W. Thiel, J. Chem. Phys. **123**, 134308 (2005).
[70] C. Moler and C. Van Loan, SIAM Rev. **45**, 3 (2003).
[71] R. M. Gester, H. C. Georg, S. Canuto, M. C. Caputo, and P. F. Provasi, J. Phys. Chem. A **113**, 14936 (2010).
[72] A. Møgelhøj, K. Aidas, K. V. Mikkelsen, S. P. A. Sauer, and J. Kongsted, J. Chem. Phys. **130**, 134508 (2009).
[73] S. P. A. Sauer and M. J. Packer, in *Computational Molecular Spectroscopy*, edited by P. R. Bunker and P. Jensen (Wiley, London, 2000), Chap. 7, pp. 221–252.
[74] N. F. Ramsey, Phys. Rev. **91**, 303 (1953).
[75] J. Linderberg and Y. Öhrn, *Propagators in Quantum Chemistry* (Academic, London, 1973).
[76] E. S. Nielsen, P. Jørgensen, and J. Oddershede, J. Chem. Phys. **73**, 6238 (1980).
[77] J. Geertsen and J. Oddershede, Chem. Phys. **90**, 301 (1984).
[78] M. J. Packer, E. K. Dalskov, T. Enevoldsen, H. J. A. Jensen, and J. Oddershede, J. Chem. Phys. **105**, 5886 (1996).
[79] K. L. Bak, H. Koch, J. Oddershede, O. Christiansen, and S. P. A. Sauer, J. Chem. Phys. **112**, 4173 (2000).
[80] B. O. Roos, in *Ab Initio Methods in Quantum Chemistry—II. Advances in Chemical Physics*, edited by K. P. Lawley (Wiley, Chichester, 1987), pp. 399–445.
[81] J. Olsen, B. O. Roos, P. Jørgensen, and H. J. A. Jensen, J. Chem. Phys. **89**, 2185 (1988).
[82] H. J. A. Jensen, P. Jørgensen, H. Ågren, and J. Olsen, J. Chem. Phys. **88**, 3834 (1988).
[83] H. J. A. Jensen, P. Jørgensen, H. Ågren, and J. Olsen, J. Chem. Phys. **89**, 5354 (1988).
[84] S. P. A. Sauer, J. Chem. Phys. **98**, 9220 (1993).
[85] M. J. Packer, E. K. Dalskov, S. P. A. Sauer, and J. Oddershede, Theor. Chim. Acta **89**, 323 (1994).
[86] DALTON, a molecular electronic structure program, Release 2.0, http://www.kjemi.uio.no/software/dalton/dalton.html, 2005.
[87] H. Koch, O. Christiansen, R. Kobayashi, P. Jørgensen, and T. Helgaker, Chem. Phys. Lett. **228**, 233 (1994).
[88] H. Koch, A. S. de Merás, T. Helgaker, and O. Christiansen, J. Chem. Phys. **104**, 4157 (1996).
[89] F. B. van Duijneveldt, IBM Technical Report No. RJ945, 1971.
[90] T. H. Dunning, Jr., J. Chem. Phys. **90**, 1007 (1989).
[91] V. Galasso, J. Mol. Struct.: THEOCHEM **93**, 201 (1983).
[92] G. Fronzoni and V. Galasso, J. Mol. Struct.: THEOCHEM **122**, 327 (1985).
[93] H. Fukui, K. Miura, H. Matsuda, and T. Baba, J. Chem. Phys. **97**, 2299 (1992).
[94] T. Helgaker, M. Watson, and N. C. Handy, J. Chem. Phys. **113**, 9402 (2000).
[95] P. Lantto and J. Vaara, J. Chem. Phys. **114**, 5482 (2001).
[96] M. Pecul and J. Sadlej, Chem. Phys. Lett. **360**, 272 (2002).
[97] T. Janowski and M. Jaszunski, Int. J. Quantum Chem. **90**, 1083 (2002).
[98] W. S. Benedict and E. K. Plyler, Can. J. Phys. **35**, 1234 (1957).
[99] See supplementary material at http://dx.doi.org/10.1063/1.3359850 for a FORTRAN routine to evaluate the $^{1}\bar{J}^{N1}$ and $^{2}\bar{J}^{23}$ values at arbitrary geometries.
[100] S. P. A. Sauer, V. Špirko, I. Paidarová, and J. Oddershede, Chem. Phys. **184**, 1 (1994).
[101] S. N. Yurchenko, R. J. Barber, A. Yachmenev, W. Thiel, P. Jensen, and J. Tennyson, J. Phys. Chem. A **113**, 11845 (2009).
[102] P. R. Bunker and P. Jensen, *Molecular Symmetry and Spectroscopy*, 2nd ed. (NRC Research, Ottawa, 1998).
[103] P. Jensen and P. R. Bunker, Mol. Phys. **97**, 821 (1999).
[104] R. D. Wigglesworth, W. T. Raynes, J. Oddershede, and S. P. A. Sauer, Mol. Phys. **96**, 1595 (1999).
[105] R. D. Wigglesworth, W. T. Raynes, S. Kirpekar, J. Oddershede, and

S. P. A. Sauer, J. Chem. Phys. **112**, 736 (2000).
[106] R. A. Bernheim and H. Batiz-Hernandez, J. Chem. Phys. **40**, 3446 (1964).
[107] W. M. Litchman, M. Alei, Jr., and A. E. Florin, J. Chem. Phys. **50**, 1897 (1969).
[108] M. Alei, A. E. Florin, W. M. Litchman, and J. F. O'Brien, J. Phys. Chem. **75**, 932 (1971).
[109] R. E. Wasylishen and J. O. Friedrich, Can. J. Chem. **65**, 2238 (1987).